

Supporting Information

Open-Source DFT Calculations of Electronic Structure to Understand Bonding in Solids

Mona Layegh, Joseph W. Bennett*

Department of Chemistry and Biochemistry, University of Maryland Baltimore County,
Baltimore, Maryland, 21250, USA. E-Mail: bennettj@umbc.edu

Table of Contents

S1. Curriculum Alignment, Prior Knowledge, Learning, and Assessment	S1
S2. Procedure for Electronic Structure and PDOS Data Generation	S5
S3. Crystal structures and supplementary electronic structure analysis	S10
S4. Step-by-Step Guide to PDOS and Band Structure Visualization	S14
S5. Input file set for PDOS and Band Analysis per Material System	S21
S6. Computational resource to run a DFT calculation	S24
S7. Reference	S27

S1. Curriculum Alignment, Prior Knowledge, Learning, and Assessment

S1.1. Curriculum placement

To further assist instructors, we outline key spots within the undergraduate and beginning graduate curriculum where these tutorials on semiconductors can be most effectively incorporated. These tutorials can be integrated into the curriculum across various undergraduate and graduate courses, as recommended:

- **First-Year Chemistry Undergraduates:** In **introductory courses**, such as "*Chemistry 2e*"¹, to introduce basic concepts in **electronic structure** after discussing **semiconductors**.
- **Physical Chemistry Undergraduates:** Ideal for inclusion after **molecular structure** and **ab initio methods**. For example, after **Chapter 16** in "*Chemical Principles: The Quest for Insight*" by **Atkins et al.**² (Freeman, 6th edition, 2013), or **Chapter 10** in "*Physical Chemistry*" by **Atkins et al.** (Freeman, 9th edition, 2010)³.
- **Inorganic Chemistry Undergraduates:** After **Chapter 7, "The Crystalline Solid State"**, in "*Inorganic Chemistry*" by **Miessler et al.**⁴ (Pearson, 5th edition, 2014), where students can explore **solid-state structure** and **electronic properties**.
- **Graduate Molecular Symmetry and Group Theory:** After completing "**Programme 8**" on **Representations** in "*Molecular Symmetry and Group Theory*" by **Vincent**⁵ (Wiley, 2nd edition, 2001), these tutorials act as a **practical application of symmetry in electronic structure**.
- **Special Topics for Advanced Undergraduates and Beginning Graduates:** In **advanced courses** such as **solid-state materials chemistry**, these tutorials can be included after **Chapter 6, "Electronic Band Structure"** in "*Solid State Materials Chemistry*" by **Woodward et al.**⁶ (Cambridge, 1st edition, 2021).

S1.2 Prior Knowledge and Additional Resources

To effectively engage with these tutorials, students should have a foundational understanding of key chemistry concepts, including chemical bonding, oxidation states, and the fundamental properties of semiconductors, which are typically covered in their introductory chemistry courses. Additionally, an overview of band theory, solid-state structure, and density functional theory (DFT) is provided in Section 2 of the main manuscript to support students' learning. For further enrichment and lesson plan content, instructors can refer to the "Further Reading" section of the Supporting Information, which includes key journal articles and books on electronic structure, chemical bonding, and DFT. These references serve as supplementary materials for lesson plans beyond the core pedagogy outlined in Section 2 of the main manuscript. More detailed instructional guidance, including a short description of the necessary input parameters for QE and data visualization techniques using XmGrace, is provided in Sections S2 and S4 of the Supporting Information for both instructors and students. **Instructors can structure lesson plans around the content provided in Sections S2, S3, S4, S5, and S6 directly using the materials available here.**

a) **Key Journal Articles and Books**

- 1) "Solids and surfaces: a chemist's view of bonding in extended structures" by Roald Hoffmann (1988) - Book⁷ (students & instructors)
- 2) "A chemical and theoretical approach to bonding at surfaces" by Roald Hoffmann (1993) - Journal Article.⁸ (students & instructors)
- 3) "How Chemistry and Physics Meet in the Solid State" by Roald Hoffmann (1987) - Journal Article⁹ (students and instructors)
- 4) "Designing meaningful density functional theory calculations in materials science—a primer" by Ann E. Mattsson, et al. (2004) - Journal Article¹⁰ (students and instructors)
- 5) "Iterative minimization techniques for *ab initio* total-energy calculations: molecular dynamics and conjugate gradients" by Michael C. Payne (1992) - Journal Article¹¹ (instructors)
- 6) "Density functional theory: a practical introduction" by David S. Sholl and Janice A. Steckel (2009) - Book¹² (advanced students, graduate students, and instructors)
- 7) "Introduction to Solid State Physics" by Charles Kittel (1976) – Book.¹³ (graduate students & instructors)
- 8) "Electronic Structure: Basic Theory and Practical Methods" by Richard Martin (2000) – Book¹⁴ (advanced students and instructors)

b) **Digital Resources**

To enhance student engagement and provide additional computational tools for exploring electronic structure and materials properties, the following digital and cloud-based resources can be recommended to form additive lessons and self-guided student exploration:

- 1) **Nanohub:** An interactive platform offering simulation tools, tutorials, and resources for semiconductor physics and DFT-based electronic structure analysis.
- 2) **Materials Project:** A widely used open-access database providing DFT-calculated properties of materials, including electronic band structures and density of states (DOS).
- 3) **Materials Cloud:** A digital hub for sharing and visualizing computational materials science data, including structural analysis and electronic properties.
- 4) **AFLOW Library:** A computational materials repository with precomputed band structures, structural data, and thermodynamic properties.
- 5) **NoMaD (Novel Materials Discovery):** A cloud-based repository for materials science data, featuring thousands of DFT-computed band structures and electronic properties.

c) Computational and Visualization Tools

- 1) **Quantum ESPRESSO:** A widely used DFT package for electronic structure calculations, accessible via cloud computing platforms and Google Colab.
- 2) **XCrySDen:** A visualization tool for electronic structure data, including band structures and charge density maps.
- 3) **VESTA:** A free software for visualizing crystal structures, electron densities, and band structures.
- 4) **ASE (Atomic Simulation Environment):** A Python-based framework for setting up, running, visualizing, and analyzing atomistic simulations.

S1.3. Pace of Instruction

We suggest allocating one week to cover the materials presented in Section 2, two lab or lecture sessions. These sessions will focus on structure-property relationships, electronic structure, and molecular orbital (MO) theory. The first lecture should introduce band theory and bonding concepts, providing the necessary theoretical foundation (Section 2 of the main manuscript). The hands-on tutorial will take place during the subsequent class/lab session, where students will apply these concepts in an interactive learning environment.

S1.4. Learning objectives and assessment

The tutorial is designed to achieve the following learning objectives:

- Plot and interpret electronic band structures and their corresponding PDOS.
- Understand the structural and electronic differences among common semiconductors
- Identify the HOMO and LUMO in the electronic band structure
- Describe the correlation between atomic bonding, electronic structure, and interaction strength.
- Explain the dispersion features in the electronic band structure of semiconductors
- Develop proficiency in using open-source tools for DFT calculations
- Establish connections between electronic band structures and atomic orbitals forming molecular orbitals.

S1.5. Assessment Methods:

Student learning can be assessed through multiple approaches:

a) **Tutorial Assessment:**

Students will analyze an **electronic band structure** and its **corresponding PDOS plot**, identifying key features. A structured **checklist** will guide them in describing:

- Material Identification: Metal, semiconductor, or insulator?
- Bonding Type: Covalent, ionic, metallic, or mixed?
- Valence and Conduction Bands: Where are VBM (HOMO) and CBM (LUMO) located?
- Band Gap: Direct or indirect? The band gap value?

- PDOS Features: Which atomic orbitals contribute (s, p, d, f)? Overlaps?
- Band Dispersion: Are bands flat (localized) or sharp (mobile carriers)?
- Structure Influence: Does symmetry affect the band structure? Any distortions?

b) Practical Task:

Students will generate at least one electronic band structure plot for the semiconductors covered in the tutorial.

c) Post-Tutorial Discussion Topics engaging students in discussions based on key semiconductor concepts include:

- **High- vs. Low-symmetry structures:** High-symmetry structures, such as cubic lattices (Si, GaAs, ZnS), result in simpler band structures due to uniform potential and bonding environments, uniform atomic sizes, and isotropic properties. These materials typically exhibit minimal band dispersion and are more likely to have direct band gaps. Lowering symmetry introduces anisotropy, varied bond lengths, and differences in ion sizes and charges, leading to complex band dispersion, indirect band gaps, and directionally dependent electronic properties. A progression from high symmetry (covalent bonding) to low symmetry (mixed ionic-covalent bonding) highlights the role of bonding in shaping electronic structure.

- **Electronegativity and ionic radii influence:** In ZnO and PbTiO₃, the directional nature of d-orbitals plays a significant role. The interaction between Zn 3d and O 2p leads to distortions that break cubic symmetry, stabilizing a hexagonal or tetragonal structure. In contrast, ZnS, with a larger, less electronegative, and more polarizable S ion compared to the O ion, weakens d-p orbital overlap, maintaining cubic symmetry.

- **Linking Bonding Complexity to Symmetry:** In contrast to semiconductors like Si or GaAs, which have higher-symmetry structures with no polar dipoles or structural asymmetry, PbTiO₃ adopts a tetragonal structure due to the polar nature of the Pb ion. This polarity arises from its lone pairs, which require structural asymmetry to stabilize the dipoles. The reduced rotational symmetry enhances anisotropic properties and supports ferroelectricity.

- **Band gap trends:** CaCO₃ (4.14 eV) > PbTiO₃ (1.70 eV) > PbO (1.32 eV) > ZnO (0.66 eV). This trend illustrates how bond number and type impact electronic properties. Materials with primarily ionic bonding, such as CaCO₃, exhibit larger band gaps, while materials like PbO and ZnO, which have a polar, mixed-bonded nature and increased orbital hybridization, exhibit smaller band gaps. In CaCO₃, the carbonate group features a double bond, with the carbon atom in a +4 oxidation state and the charge distributed across the carbonate unit, contributing to its high band gap. In contrast, PbTiO₃ has a mix of ionic and covalent character, with six bonds to the central Ti atom in a +4 oxidation state, resulting in a smaller band gap.

S2. Procedure for Electronic Structure and PDOS Data Generation

This section provides a detailed explanation of the steps involved in the PDOS and band structure calculation flowchart, as illustrated in Figure 2 of the manuscript.

S2.1. ICSD - Initial Structural Data

The process begins by accessing the Inorganic Crystal Structure Database (**ICSD**) website to get the raw structural data by downloading Crystallographic Information Files (**CIFs**) which include detailed information about atomic positions, lattice parameters, and symmetry properties essential for simulation preparation. Other open source options for crystallographic data include the Crystallography Open Database^{15,16} (www.crystallography.net) and the Materials Project¹⁷ (www.materialsproject.org). The data used as input structures can be high-quality, experimentally measured under atmospheric pressure and at room temperature, though some differences will be present when compared to DFT simulations performed at 0 K. Using visualized CIF files¹⁸, we can examine the structural properties such as atomic arrangement, bond length, symmetry, etc. before running calculations. VESTA¹⁹ (open source: www.jpm-minerals.org), XCrySDen²⁰ (open source: www.xcrysden.org), and CrystalMaker²¹ (www.crystalmaker.com) are useful graphical software for this purpose. XCrySDen is especially advantageous for Quantum ESPRESSO users because it supports direct and easy opening of input and output files. Additionally, it serves as an intermediary tool to convert input and output files into formats compatible with other graphical software.

S2.2. vc-relax: Structural Optimization

The experimental structural data from the ICSD requires subsequent geometry optimization to reach the lowest energy state and align with DFT's force conditions and internal energy expectations for computational accuracy. Variable cell (vc) structural relaxation iteratively refines geometrical atomic positions and lattice configuration to minimize internal stress and forces. The optimized atomic positions and lattice parameters in the vc-relax output file becomes the starting point for further electronic structure calculations.

To run a vc-relax calculation, the following components are required: PSP files, pw.x executable file, runscript, and input file. **pw.x** is the main QE tool for plane-wave calculations, including vc-relax. It optimizes atomic positions and lattice parameters to minimize the total energy of lattice configuration. The **runscript** manages pw.x execution, input/output flow for multiple calculations. It is an essential file while running calculation on computing clusters. Figure S1 illustrates an example **vc-relax QE input file**. Each separate section, denoted with an ampersand (&), controls a different part of the calculation.

To complement the definitions provided by Quantum Espresso, in the next few sections a focus is placed on describing the input parameters that ultimately govern electronic band structure calculations workflow. The following discussion outlines the key parameters and their roles in the setup:

a) &CONTROL

- **calculation**: defines the type of calculation. Here, “vc-relax” means the calculation optimizes both lattice parameters and atomic positions at the same time (vc is variable cell).
- **prefix**: A label used to name output files, here set as 'Si' for silicon. This parameter helps to organize files under a common prefix.
- **pseudo_dir**: Directory of pseudopotential files.
- **outdir**: Directory in which output files will be saved.

- **etot_conv_thr** and **forc_conv_thr**: Convergence thresholds for total energy and atomic forces, respectively, defining the accuracy criteria. It means the calculation will stop iterating once the change in total energy between steps falls below the convergence threshold limit.
- **nstep**: Maximum number of iterations for the relaxation process. It is a restricting parameter to the relaxation iterations. If the convergence occurs earlier, the calculation will be stopped.

```

a) &CONTROL
    calculation = 'vc-relax',
    prefix = 'Si',
    pseudo_dir = './',
    outdir = './',
    etot_conv_thr=1.D-7,
    forc_conv_thr=2.D-6,
    nstep=150,
/
b) &SYSTEM
    ibrav = 2,
    celldm(1) = 10.26221 ,
    nat = 8,
    ntyp = 1,
    ecutwfc = 40,
    ecutrho = 320,
    occupations = 'smearing',
    smearing = 'gaussian',
    degauss = 0.02,
    input_dft = 'WC',
/
c) &ELECTRONS
    electron_maxstep = 150,
    diagonalization = 'david',
    conv_thr = 1.0d-7,
    mixing_beta = 0.20,

```

```

d) /
  &IONS
  /
  &CELL
    press = 0.0,
  /
e) ATOMIC_SPECIES
    Si 28.0855 si_pbe_v1.uspp.F.UPF
  ATOMIC_POSITIONS (crystal)
    Si   0.125   0.125   0.125
    Si   0.125   0.625   0.625
    Si   0.625   0.125   0.625
    Si   0.625   0.625   0.125
    Si   0.875   0.375   0.375
    Si   0.875   0.875   0.875
    Si   0.375   0.375   0.875
    Si   0.375   0.875   0.375
f) K_POINTS {automatic}
    10 10 10 0 0 0

```

Figure S1. An example of a variable cell structural relaxation input file for Si.

b) &SYSTEM

- **ibrav**: defines which of the 14 unique Bravais lattice types applies to the crystal in the QE input file, minimizing input complexity. For example, ibrav = 2 represents a face-centered cubic (FCC) lattice. With a specified ibrav value, QoB-E automatically uses the related lattice vectors (a , b , and c) and angles between them (α , β , γ).
- **celldm()**: defines the size of unit cell in Bohr units. It is one of the key parameters which determines the size for the overall crystal structure.
- **nat and ntyp** : gives the total number of atoms and the number of unique atomic species in the unit cell, respectively.
- **ecutwfc** and **ecutrho**: control the wavefunction and charge density cutoff energies. The cutoff energy decides which planewaves are included in the basis set by controlling the kinetic energy upper limit. **ecutrho** is typically between 4-12 times larger than **ecutwfc** because charge density demands finer detail for accuracy.
- **occupations**: sets the method for electron distribution among energy states in the system. "fixed" for insulators or "smearing" for metals are common ones to improve convergence.
- **smearing**: evenly distributes electrons across energy levels. It applies to the systems with partial band occupancy, mainly metallic systems, leading to smoother and more convergent calculations.
- **degauss**: determines how much partial electron occupancies spread in systems using smearing.
- **input_dft**: defines the exchange-correlation functional used in calculations. "WC" here denotes the Wu-Cohen GGA functional.

c) &ELECTRONS

- **electron_maxstep**: sets the limit on the number of calculations for reaching a stable electron configuration within the system.
- **diagonalization**: determines the method for calculating the energy levels of electrons in a system, with speed and accuracy varying by method. "david" is often chosen for accuracy, while "cg" offers greater efficiency.
- **conv_thr**: sets the threshold for the energy change that determines when the calculation stops. The energy change refers to differences in total energy between calculation steps as the electron configuration stabilizes in the material.
- **mixing_beta**: defines the factor for mixing electronic densities between consecutive iterations during self-consistent field (SCF) calculations.

d) &IONS and &CELL

The &IONS section handles ionic relaxation parameters, with additional parameters for controlling the ion movements if necessary. The &CELL section deals with volume and pressure settings. In this example, press=0 sets the external pressure to zero.

1. ATOMIC_SPECIES and ATOMIC_POSITIONS

- **ATOMIC_SPECIES** lists the atomic types present in the unit cell with their atomic masses and corresponding PSP files.
 - **ATOMIC_POSITIONS**, typically derived from ICSD, lists the positions of each atom in the unit cell in fractional coordinates before relaxation.
2. **K_POINTS**: determines how the Brillouin zone is sampled. It can be considered as another parameter to balance speed and precision in calculations. Here, 10 10 10 0 0 0 means a $10 \times 10 \times 10$ grid with no shifts.

S2.3. Band structure and PDOS calculations

This section provides a detailed overview of the band structure and PDOS calculations, using the optimized structure obtained in section 3.2. For a PDOS and band structure calculation, various executables, as summarized in Table S1, are used to perform SCF, NSCF, band structure, and DOS calculations.

Table S1. Overview of programs, inputs, and outputs for electronic structure and DOS calculations

Executable	Input	Output					
pw.x	scf.in						scf.out
	nscf.in						nscf.out
	bands.in						bands.out
projwfc.x	pdos.in	pdos.out	pdos_tot				"filpdos".pdos_atm#N(X)_wfc#M(l)
dos.x	dos.in		dos.out				dos.dat
bands.x	bands.in	bands.dat	bands.dat.rap	bands.dat.gnu	bands.out	bands.ps	
plotband.x	plotband.in			plotband.out			

The workflow starts with **pw.x** to generate electron density and band structure data, followed by **projwfc.x** and **dos.x** for analyzing atomic orbital contributions (PDOS) and total DOS. **bands.x** and **plotband.x** are then employed to create different file formats to facilitate plotting and visualization of the band structure.

a) **pw.x: SCF, NSCF, and Band structure calculations**

As explained at the beginning of section 3, the **SCF calculation** determines ground state electron density of a material by iteratively solving the KS equations until convergence. The result of this step is used for consequent calculations. The **Non-Self-Consistent Field (NSCF)** calculation is the next on the list. Without recalculating the electron density, NSCF uses the obtained electron density by the SCF calculation to compute the electronic states at a denser k-point grid, preparing for a higher resolution band structure analysis. **Band Structure Calculation** performed by the same **pw.x** executable, the bands.in step, using the electron density generated from the SCF step, computes the electronic band structure along a path with selected high-symmetry points **in the Brillouin zone** for visualized analysis. The input files for all three calculations are quite similar to those used for vc-relax calculations with some minor difference:

- **nbnd Parameter:** is added to the **&SYSTEM** section which presents the number of electronic states (bands) to be calculated. If the system is insulator, the default value is the number of valence bands (number of electrons divided by two) and if the system is metallic, it should be number of valence bands plus an additional 20% to account for conduction bands.
- **Calculation Mode:** calculation= ‘**scf**’ for SCF file. calculation= ‘**nscf**’ for NSCF file. calculation= ‘**bands**’ for Bands file.
- **k-Point Grid:** a denser k-point grid in the **NSCF file** compared to scf and vc relax files for a more detailed result. **Bands** calculation, uses a custom k-point path along high-symmetry points in the Brillouin zone to map out the band structure. This k-point path in the reciprocal lattice matches the symmetry of the crystal using standard labels from crystallography. According to the crystal symmetry of the system under study, the recommended high-symmetry k-point path for that symmetry can be found in the literature ^{22,23}.
- **The output files** contain key information for analyzing the electronic properties of materials and performing subsequent calculations. The **SCF output** specifies the converged electron density, total energy, Fermi energy of the system and atomic forces. The **NSCF output** provides detailed eigenvalues and wavefunctions across a denser k-point grid, required for more refined energy bands. The **bands output** gives eigenvalues at each k-point along the high symmetry path in the Brillouin zone. This provides the key dataset for plotting the electronic band structure, and identifying the E_g for insulators and semiconductors. Key information from each output file will be highlighted in Section 4, but all users are encouraged to go through the output log files in greater detail.

b) projwfc.x, dos.x: PDOS and DOS calculations

After pw.x calculations (SCF, NSCF, bands), further analysis can focus on density of states with **projwfc.x**, for orbital contributions, and **dos.x**, for the total DOS related to electronic state distribution across energy levels. Both calculations use NSCF output wavefunction and eigenvalues data for processing density of states information. Both **input files** contain basic parameters. The PDOS input defines the output directory (outdir), prefix (prefix), and step size (DeltaE). DeltaE sets the energy increment defining the resolution of energy distribution information. The DOS input includes the energy limits (Emin, Emax), DeltaE, output directory, and filename (fildos).

Projwfc.x calculation results are stored by specified **output files**. **pdos.out** can be considered as an overview of **pdos_tot**. In pdos_tot, the total PDOS data for all atoms and orbitals in the unit cell in the specified energy range is included, while in **pdos.out** information about parameters, method, summary of total PDOS values, convergence and warnings are included. Atomic PDOS by atom and orbital type is stored in files like **filpdos.pdos_atm#N(X)_wfc#M(l)**, where N, X, and l represent the atom number, symbol, and orbital type (s, p, d, f), respectively. These files are generated per atomic wavefunction in the pseudopotential file and are used to plot PDOS for individual atomic orbitals in a material. For example, Si.pdos_atm#1(Si)_wfc#2(p) contains PDOS data for the p orbital ($l=1$) of the Si atom labeled by number 1. Each file is composed of columns arranged as follows:

- **E (eV)**: energy of the orbital in eV.
- **ldos(E)**: the total DOS for a particular orbital by summing contributions from each orbital component.
- **pdos(E)** Columns: is the DOS projected onto each component. ldos (E) is calculated by summing these pdos(E) values. The order of orbital components columns appears as: $p_z - p_x - p_y$ (for a p-orbital) and $d_{z^2} - d_{zx} - d_{zy} - d_{x^2-y^2} - d_{xy}$ (for a d-orbital).

This means that an **s-orbital pdos** file has three columns, a **p-orbital** pdos file has five columns, and a **d-orbital pdos** file has seven columns. In spin-polarized cases, atoms with unpaired d-orbitals, each **pdos(E)** and **ldos(E)** entry has separate columns for spin-up and spin-down components, doubling the number of columns.

c) bands.x, plotband.x

The **bands.x** executable program reads the raw data generated by **pw.x** in calculation = 'bands' mode (section 3.3.a). The **bands.in** file includes information about prefix to align with pw.x input files, filband for output naming, and outdir to locate the directory where these data are stored. It formats and reorder the band structure information, producing various output files for visualization.

bands.dat contains the band structure in a format with re-ordered bands suitable for plotting code "plotband.x". **bands.dat.rap** (with symmetry information) contains raw data for custom plotting, **bands.dat.gnu** format prepared for Gnuplot visualization, **bands.ps** plots band structure immediately in PostScript format. **bands.out** is the log file for bands.x and includes additional details on calculated properties, summarizing any band properties computed.

S2.4. Data visualization

The PDOS-Band graph can be presented in a two-panel setup, with the left panel displaying the band structure using data from **bands.dat.gnu**. The right panel visualizes the distinct density of states contributions from each atom and orbital, using **filpdos.pdos_atm#N(X)_wfc#M(l)** pdos files. In this study, we used open source **XmGrace** package to plot the Bands-PDOS graphs. **XmGrace** is designed specifically for Unix-based systems like Linux, macOS with XQuartz for GUI support or on clusters for remote users.

XmGrace is the graphical version of **Grace** which is also developed for Unix-based systems, including Linux and macOS. XmGrace is not available on Windows but it can be run via **Cygwin**. For Windows users, there are some alternative options like: **OriginPro** which is an advanced licensed software for advanced plotting capabilities. Gnuplot^{24,25} is free and works well for plotting these graphs but might be challenging to learn. Matplotlib is python plotting library that offers high-quality customizable plots for users with coding background.

S3. Crystal structure and supplemental electronic structure analysis

Table S2 provides an overview of lattice constants and key electronic structure parameters for all seven system of materials. This table highlights differences between experimentally measured and DFT-calculated lattice constants, along with essential electronic properties such as the minimum energy level in the conduction band and the maximum energy level in the valance band. These values are fundamental to band structure analysis. While the main article already covers the four primary semiconductor and oxide system, this section focuses on the remaining three complex oxides: PbO, PbTiO₃, and CaCO₃, providing PDOS and band structure analysis, along with unit cell structure and bonding characteristics.

Table S2. A brief review of compounds in this study.

Compound	Lattice Constant (Å) ICSD	Lattice Constant (Å) DFT	E _v (eV)	E _c (eV)	E _f (eV)	E _g (eV)
Si	$a = b = c = 5.43$	$a = b = c = 5.74$	6.10	6.57	6.33	0.47
GaAs	$a = b = c = 5.65$	$a = b = c = 5.66$	7.11	7.48	7.30	0.37
ZnS	$a = b = c = 5.41$	$a = b = c = 5.36$	6.98	8.99	8.05	2.01
ZnO	$a = b = 3.25, c = 5.21$	$a = b = 3.24, c = 5.23$	8.69	9.35	9.18	0.66
PbO	$a = b = 3.98, c = 5.02$	$a = b = 3.99, c = 5.03$	8.49	9.81	9.28	1.32
PbTiO₃	$a = b = 3.90, c = 4.15$	$a = b = 3.87, c = 4.21$	10.4 5	12.1 4	11.2 5	1.69
CaCO₃	$a = 5.74, b = 4.96, c = 7.97$	$a = 5.67, b = 4.95, c = 7.93$	5.93	10.0	7.50	4.14

S3.1. PbO (Litharge)

Litharge, also known as lead monoxide (PbO), crystallizes in a tetragonal layered structure. As shown in Figure S2.a, each lead (Pb) atom is bonded with four oxygen (O) atoms and each oxygen atom is also bonded to four lead atoms under a mixture of ionic and covalent bonding character and equal Pb—O bond lengths of 2.32 Å, indicative of strong interaction between the ions. This square planar arrangement creates a layered structure. The lattice parameters for litharge are typically around $a = b = 3.98 \text{ \AA}$ and $c = 5.02 \text{ \AA}$. The symmetry of the litharge crystal structure belongs to the centrosymmetric space group P4/nmm, which is known as a high degree of symmetry for tetragonal crystals^{26,27}.

The band structure of litharge provides insights into its semiconductive behavior of litharge with an indirect E_g , with the VBM and CBM located at the Γ point and the M Point, respectively. The calculated E_g from the graph is approximately 1.32 eV, which is lower than the indirect E_g empirical value of around 1.95 eV²⁸ due to the typical underestimation of E_g s in DFT calculations.

The PDOS plot illustrates that near Fermi level, cationic Pb 6p orbitals predominantly occupy states in the conduction band region while anionic O 2p orbitals are mainly contributing to the bonding and valence band structure of litharge. In the valence band, the interaction between Pb 6s, Pb 6p, and O 2p states represents a mixed bonding characters in a way that ionic Pb-O bonding (due to charge transfer) is partially balanced by covalent overlap of Pb 6p and O 2p orbitals. In the conduction band, the Pb 6p orbitals play a key role, with some hybridization with O 2p states.

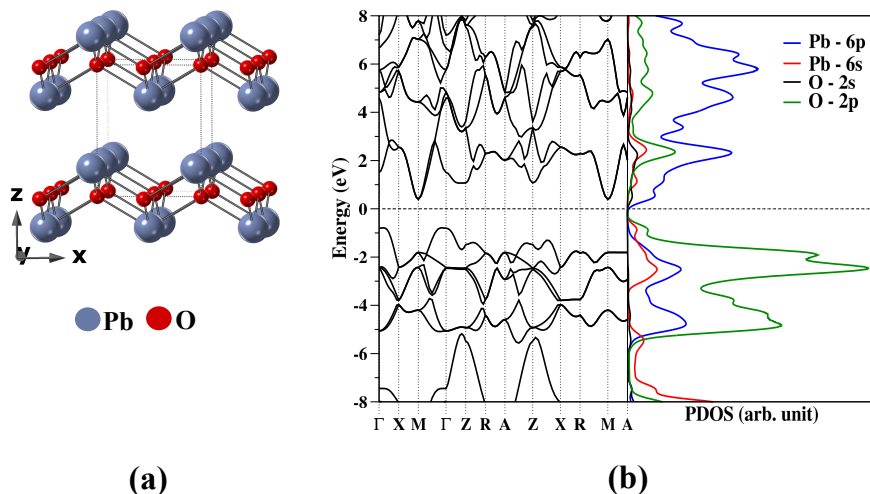


Figure S2. PbO Band structure and PDOS

Overall, the presence of well-defined peaks of O 2p and Pb 6p is indicative of strong ionic bonding character which can be also an explanation of litharge being the most energetically favorable and thermodynamically stable phase of lead oxide. Additionally, despite the dispersive nature of the bands, at core energy levels, the overlap between Pb and O orbital is indicative of covalent bonding^{28,29}.

S3.2. PbTiO₃ Tetragonal ABO₃

PbTiO₃ is a ferroelectric ABO₃ perovskite solid known for its strong polarization. It crystallizes in the polar tetragonal P4mm (99) space group with lattice parameters of $a=b=3.90$, and $c=4.15$ Å. Ferroelectrics are unique materials that possess an internal electric dipole even in the absence of electric field. Additionally, the direction of this internal dipole can be reversed in the presence of an external electric field³⁰⁻³². As shown in Figure S3.a, the unit cell features a large Pb²⁺ cation at the corner and a smaller Ti⁴⁺ cation at the center surrounded by oxygen anions. There are two inequivalent oxygen (O²⁻) sites. In the first site, O²⁻ is coordinated to two equivalent Ti⁴⁺ and two equivalent Pb²⁺ atoms. However, in the second site, O²⁻ is bonded in a distorted single-bond geometry to two equivalent Ti⁴⁺ and four equivalent Pb²⁺ atoms. Consequently, Ti⁴⁺ is surrounded by six O²⁻ atoms in an octahedral geometry with Ti—O distances ranging from 1.39 to 2.76 Å. Forming a distorted 8-coordinate geometry, Pb²⁺ is bonded to eight O²⁻ atoms with four shorter, 2.55 Å, and four longer, 2.81 Å, Pb—O bond lengths. This configuration features the complex bonding environment within the PbTiO₃ structure^{33,34}.

As shown in Figure S3, the tetragonal phase of PbTiO_3 exhibits an indirect E_g with the VBM at the X point and CBM located at the Γ/Z point. The calculated E_g value from the graph is approximately 1.69 eV, which underestimates the experimentally measured E_g (~ 3.4 eV)³⁵ due to the reasons previously mentioned. The valence band area is primarily dominated by O 2p states. Closer to VBM area, a strong hybridization of O 2p with the Pb 6s orbitals can be seen. The Ti 3d states also strongly hybridize with both O 2p and Pb 6p states. However, Ti 3d orbitals play the main role in the conduction band region, particularly near the Fermi level (CBM area). Pb 6p states contribute primarily at higher energy levels in the conduction band, hybridizing with surrounding O 2p states. It can be concluded that band structure of PbTiO_3 is largely influenced by the Ti 3d - O 2p hybridization and Pb orbitals play the secondary role, further from the E_g area.

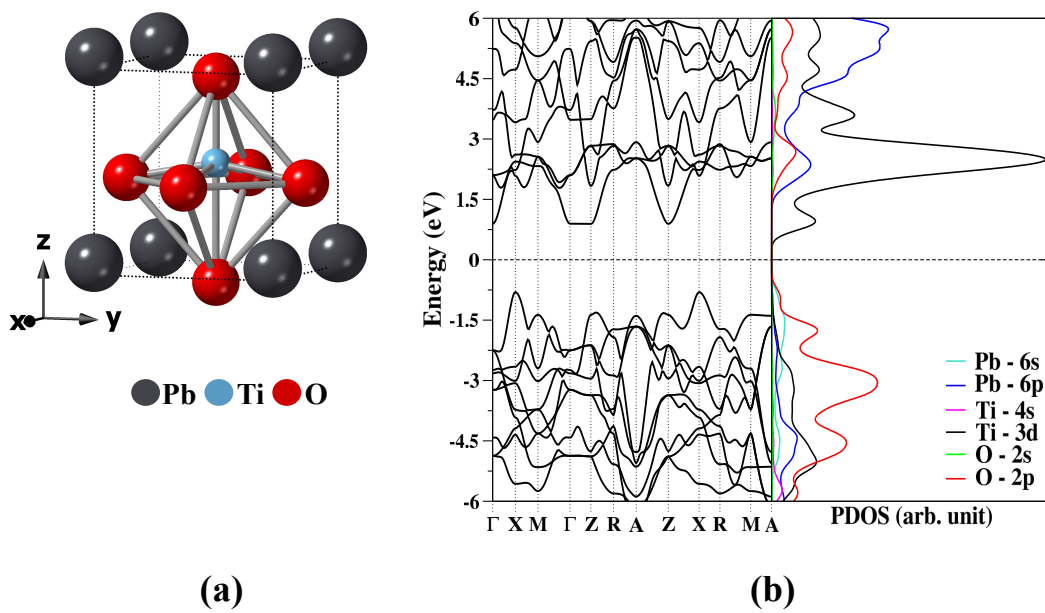


Figure S3. PbTiO_3 (a) Unit cell, (b) PDOS- Band structure.

The asymmetrical band structure patterns around the Fermi level in the conduction band region arise from variations in orbital overlap, as reflected in the PDOS plot. This behavior is a consequence of the non-centrosymmetric nature of PbTiO_3 . The PDOS plot is also a good guide to find out the origin of the strong polarization and ferroelectricity in PbTiO_3 . Focusing on the Ti—O cage surrounded by Pb ions and examining the PDOS plot near the VBM reveals covalent bonding between Pb 6p – O 2p and Ti 3d – O 2p states. The ionic core Pb–O repulsion is weakened by the covalent Pb 6p — O 2p bonds, resulting in displacement of Ti ions and lower non-centrosymmetric symmetry state³⁰.

S3.3. CaCO_3 (Aragonite)

Calcium carbonate can be found in three primary phases called Calcite (trigonal), Aragonite (orthorhombic) and Vaterite (hexagonal). Here, we look at the characteristics of Aragonite phase with a focus on the electronic band structure and PDOS properties. The primitive cell of Aragonite phase includes 20 atoms whose structure is classified in space group 62 (Pnma) with orthorhombic crystal symmetry. The aragonite phase has an orthorhombic centrosymmetric

crystal structure, as shown in the left panel of Figure S4.a, with a layered arrangement where each calcium, carbon, and oxygen atom contribute to forming planar units.

Ca atoms are stuffed between carbonate groups, while Ca atoms are located at the center of each carbonate group, forming trigonal planar CO_3 units with oxygen atoms. This creates a stabilized structure bonded by the ionic and covalent interactions between Ca^{2+} ions and the CO_3^{2-} groups, ionic for Ca-O and covalent for the CO_3 unit. In this configuration, there are nine Ca-O and three C-O bonds ranges from 2.38 to 2.53 Å and 1.28 to 1.30 Å, respectively^{36,37}. The experimental lattice parameters are reported to be $a = 5.74 \text{ \AA}$, $b = 4.96 \text{ \AA}$, and $c = 7.97 \text{ \AA}$ and our DFT-optimized results are $a = 5.66 \text{ \AA}$, $b = 4.95 \text{ \AA}$, and $c = 7.93 \text{ \AA}$ which is in a good agreement^{38,39}. In this structure, C^{4+} is covalently bonded in a planar trigonal geometry to three O^{2-} atoms forming the carbonate (CO_3^{2-}) group. Ca^{2+} ions form a two-layered close packed structure coordinated by CO_3^{2-} groups through ionic bonding. The Ca atoms are situated in distorted tricapped trigonal prism and are nine-coordinated with oxygen atoms. The distortion in the polyhedral structure and high coordination number of oxygen optimizes the stability by minimization of the repulsion between cations (Ca^{2+}) and anions (CO_3^{2-}).

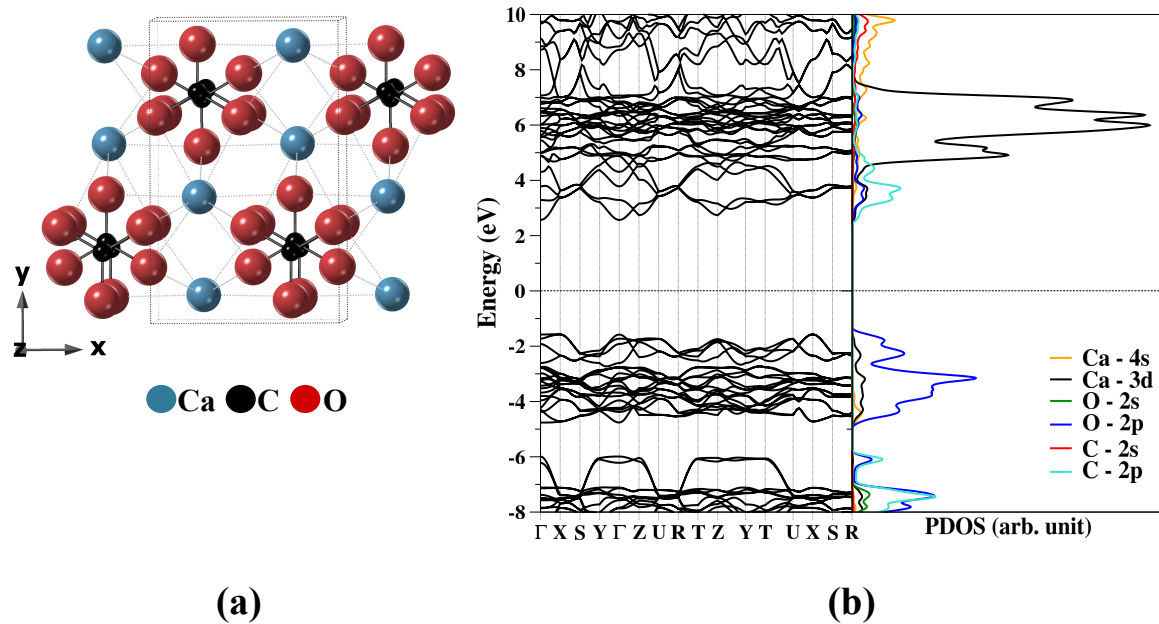


Figure S4. CaCO_3 (a) Unit cell, (b) PDOS- Band structure.

The electronic band structure of aragonite exhibits an indirect E_g of 4.14 eV with the effective VBM is degenerate at the Γ and X points and CBM located at the Γ -point. In the valence band region, the plot indicates a strong presence of O 2p states with an anionic character, which dominate this area, suggesting that oxygen plays a substantial role in the bonding within CaCO_3 , particularly in its interaction with carbon and calcium. This is followed by a smaller share of Ca 4s and Ca 3d. The lower energy (more negative) area belongs to a mixture contribution of C 2p and O 2p orbitals and the overlap of states indicates the hybridization of C 2p with O 2p states which creates strong bonding states. In CO_3^{2-} , the C with 4+ oxidation state balances the three oxygens which leads to several resonance structures, delocalization of the electrons and partial double band character. In this situation, the C 2p orbitals are engaged in multiple bonding interactions, leading to the formation of bonding and anti-bonding molecular orbital. In the conduction band, the lowest unoccupied states primarily belong to C 2p orbitals followed by Ca

3d and O 2p overlap with antibonding character. This highlights the significant role of carbon in conduction. The antibonding character of Ca 3d and O 2p overlap implies that electrons in these states weaken Ca–O bonds, affecting stability at higher energy levels. Moving further up in energy, the PDOS shows a prominent peak for the unfilled Ca 3d orbitals and a less pronounced peak of the unfilled Ca 4s states in higher energy area.

S4. Step-by-Step Guide to PDOS and Band Structure Visualization

To plot both the PDOS and band structure in the same figure, as in Figures 3-6 of the main text, we need to create two panels in one figure using XmGrace. The right panel will display the PDOS, and the left panel will show the band structure.

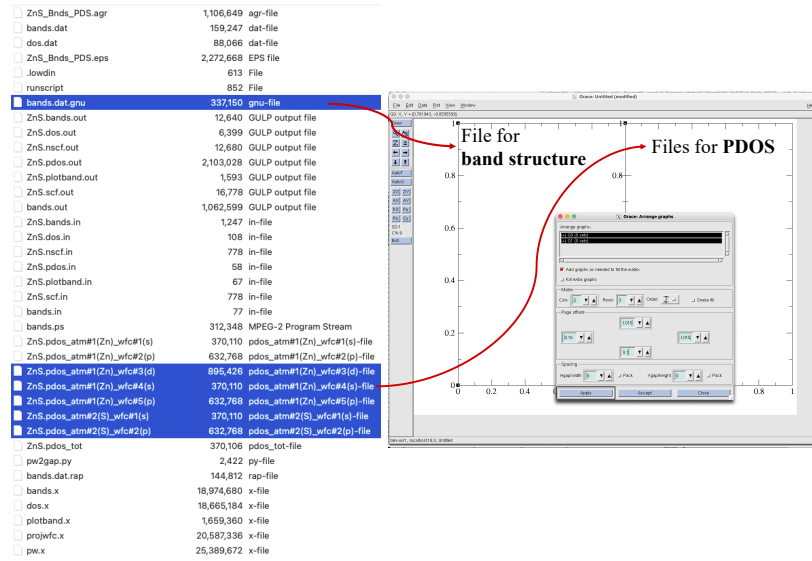


Figure S5. data files used to plot PDOS and band structure.

S.4.1 Arranging PDOS and band structure graphs using input files:

As mentioned earlier in S.1.4, the PDOS-Band graph is presented in a two-panel setup: the left panel displays the band structure using data from bands.dat.gnu, while the right panel shows the projected density of states (PDOS) contributions from each atom and orbital, based on filpdos.pdos_atm#N(X)_wfc#M(l) files (Figure S5).

To organize the panels:

1. Navigate to Edit → Arrange graphs in XmGrace.
2. In the displayed box, you will find all the options required to set the size and spacing for the panels within the figure.

S.4.2. Steps for plotting the band structure using band.dat.gnu:

To begin, we will first focus on the left panel to plot the band structure. For this, we need the related dataset, typically in the form of a **.gnu file** generated from the calculations.

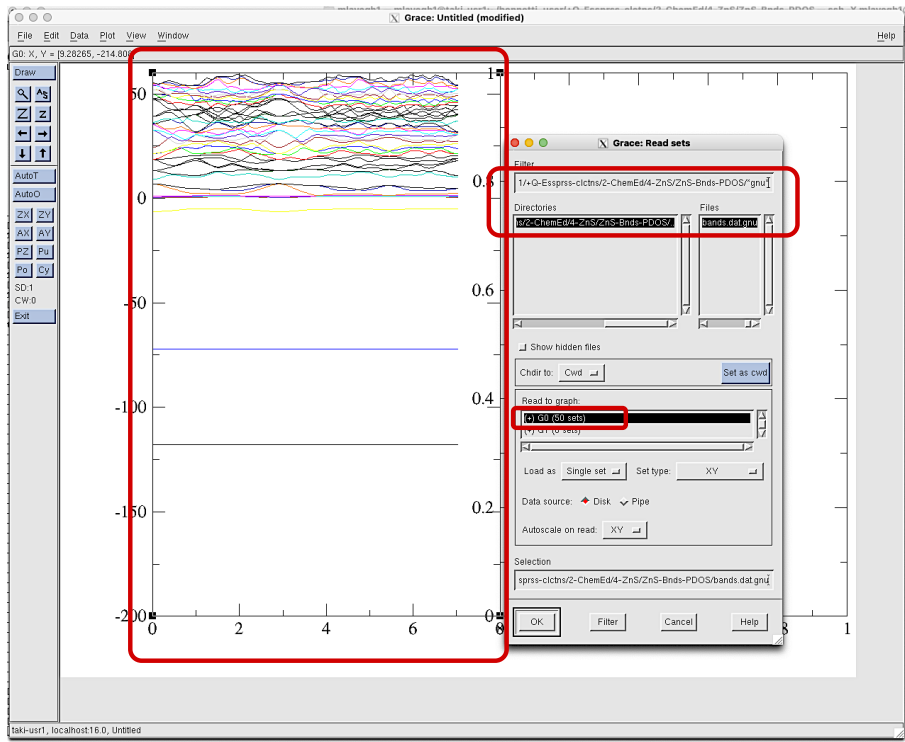


Figure S6. Importing band structure data

Importing the data file:

1. Go to Data → Import → ASCII in XmGrace.
2. In the Filter box, type *gnu* to filter the files, so the band.dat.gnu file appears in the Files box (Figure S6).
3. Select band.dat.gnu and click OK.
4. The data for the band structure will now be displayed in the G0 plot box (left panel).

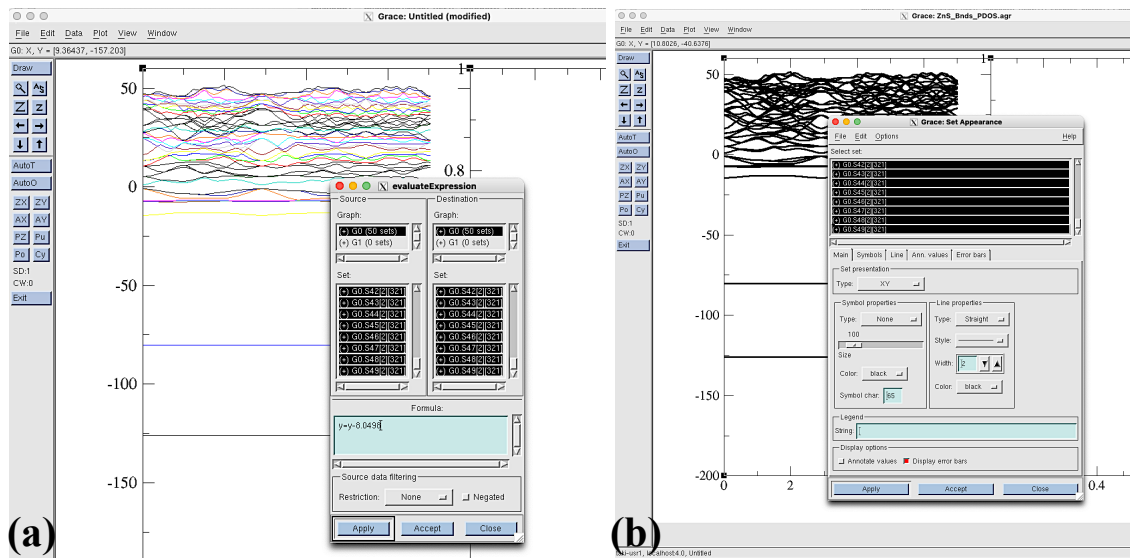


Figure S7. (a) Zero the Fermi level. (b) Editing graph's appearance.

Before plotting the band structure, ensure you have the Fermi energy value from the **scf.out** file. To find this:

Run the following command in the terminal:

```
grep "Fermi" ZnS.scf.out
```

The output will look something like this:

the Fermi energy is 8.0498 eV.

Zero the Fermi level in the plot (Figure S7.a)

Follow these steps:

1. Go to **Data → Transformations → Evaluate Expression** in xmgrace.
2. Select **all datasets** in both the **Source** and **Destination** boxes.
3. In the **Formula** box, type:

$$y = y - E_f$$

4. Replace E_f with the actual Fermi energy value (e.g., 8.0498).

5. Click **Apply**.

Avoid clicking Apply multiple times, as this will shift the bands repeatedly.

Enhancing the graph's appearance (Figure S7.b)

- Adjusting the color and size of the bands:

1. Click on any part of the graph where the bands are visible to open the “Set Appearance” window
2. In the “Select Set” box, select **all datasets** to apply the changes to all bands.
3. In the **Main → Line properties** section:
4. Set the **width** to 2.
5. Change the **color** to **black**.
6. Click **Apply** to update the figure.

The changes will be applied immediately and reflected in the graph.

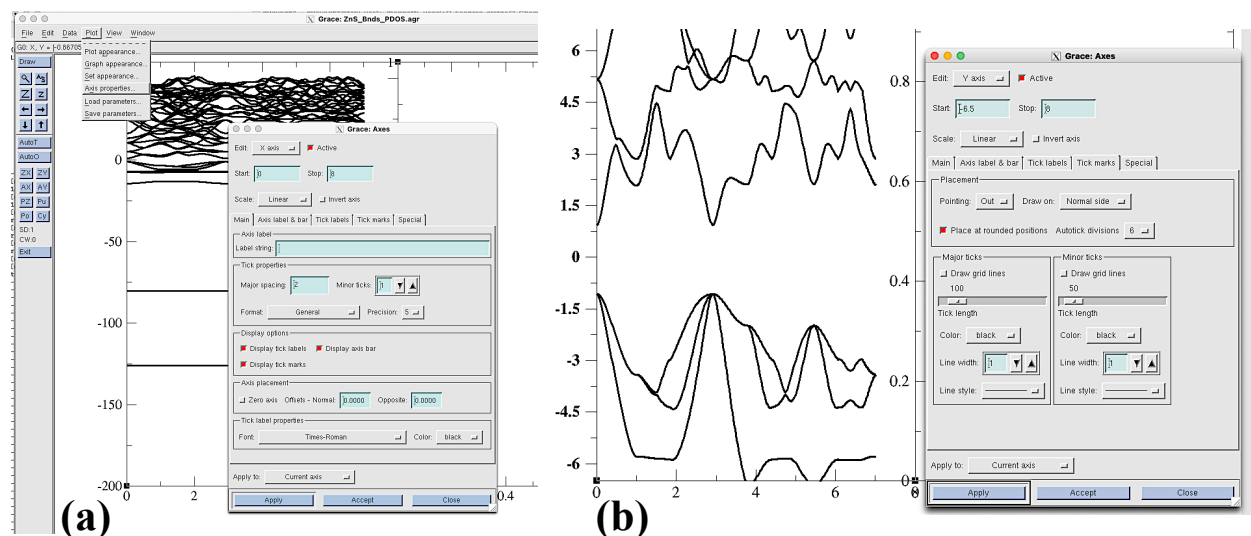


Figure S8. (a) Axes properties, (b) Setting the energy range on Y-axis.

Axes Properties (Figure S8)

To refine the **y-axis** appearance, follow these steps:

Go to **Plot → Axis Properties** and adjust the **y-axis**:

1. **Main Window:** Start = -6.5, Stop = 8, Label = Energy (eV), Major spacing = 1.5, Font = Times Bold.
 2. **Axis Label & Bar:** Font = Times-Bold, Char size = 175.
 3. **Tick Marks:** Pointing = Out, Draw on = Normal side.
 4. Click **Apply**.

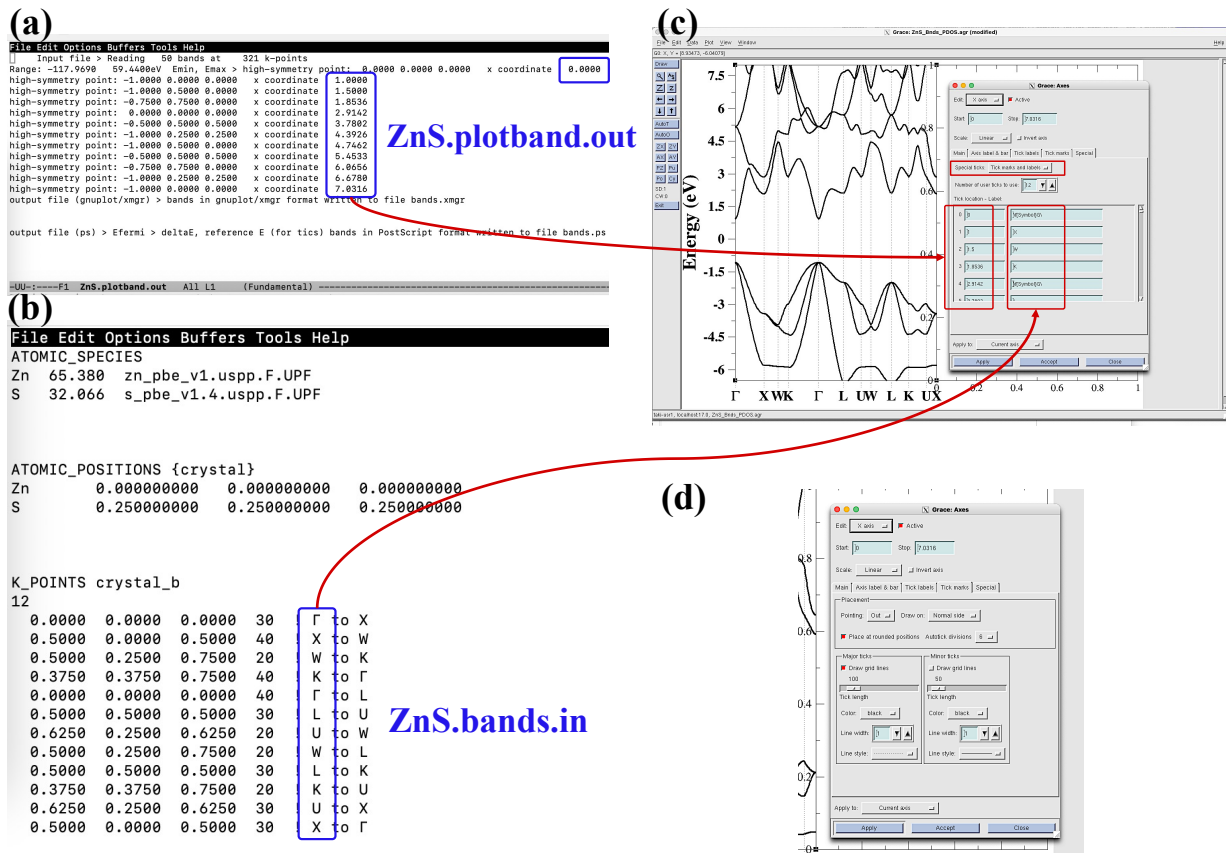


Figure S9. (a) plotband.out file, (b) ZnS.bands.in file, (c) Label the X-Axis on the band structure plot, (d) draw grid lines on high-symmetry k-points.

Instructions to Label the X-Axis on the Band Structure Plot (Figure S9)

1. Go to Plot → **Axis Properties** from the top menu.
 2. Select **X Axis** and navigate to the “**Special**” tab.
 3. For the “**Special ticks**” select: “**Tick marks and labels**”
 4. In the Tick Location - Label section:
 - Use the **plotbnd.out file** to enter the x-coordinates of your k-points under Tick Location as guided in Figure S9.a,c.
 - Label each k-point (Γ , X, etc.) based on the ZnS.**bands.in file**. (shown in Figure S9.b,c)
 - Ensure the number of ticks matches the number of high-symmetry points in your k-path.
 - The **number of user ticks to use** should be equaled to the number of high-symmetry point which here is 12.
 5. Set the **Stop value** to the final k-point.
(For ZnS, use 7.0316)
 6. Click **Apply** to finalize the changes

Using gridlines to highlight high-symmetry k-points

As shown in Figure S.9.d, we can highlight high-symmetry k-points for better band structure visualization.

1. Go to “**Tick marks**” tab
2. Enable **Draw Grid Lines** under **Major Ticks** and adjust line width/color.
3. Click **Apply**.

S.4.3. Plotting the PDOS on the right panel:

Now, we shift to the right panel to plot the PDOS, following similar steps used for the band structure plotting:

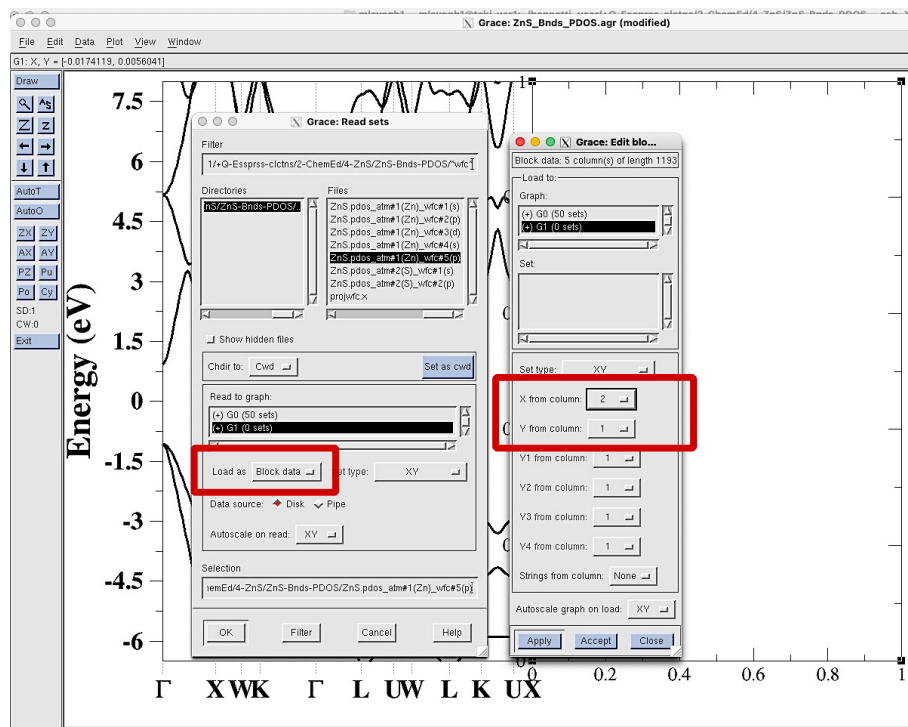


Figure S10. Importing orbital wavefunction data for plot PDOS (right panel)

1. To import the data files which are orbital wavefunctions here:

Data → Import → ASCII

In the Filter box, type ***wfc*** to display all wavefunction files.

2. Ensure data files are loaded as **Block Data** before transferring. (as demonstrated in Figure S10)
3. Load Data for Each Orbital:
4. Start with the Zinc p orbital, select the file, and click OK.
5. In the Edit Block Data window (as demonstrated in Figure S10):
 - Set the X-axis to column 2 (density).
 - Set the Y-axis to column 1 (energy).

7. Click Apply.
6. Repeat this process for all other orbital wavefunctions to be plotted.
7. Zero the Fermi Level: Repeat the same steps used for band structure:
 Data → Transformations → Evaluate Expression.
 Select all datasets in both Source and Destination boxes.
 In the formula box, type: $y = y - E_f$, using the Fermi energy (e.g., 8.0498 eV).

Click Apply.

Editing PDOS Curves and Legends (Figure S11)

1. Label PDOS Curves (Figure S11.a):
 ○ Click on the PDOS curves to open the Set Appearance box.
 ○ Navigate to Main → Legend: String and type the orbital name (here: S – 3p).
2. Edit Legend Box (Figure S11.b)
 ○ Go to Plot → Graph Appearance → **Leg. Box** and **Legends** tabs
 ○ Customize the legend box (font type, size, color, frame size, line, etc.) using the available options.
3. Edit Axes Properties:
 ○ Similar to the band structure plot, go to **Plot** → **Graph Appearance** to adjust the axis settings.

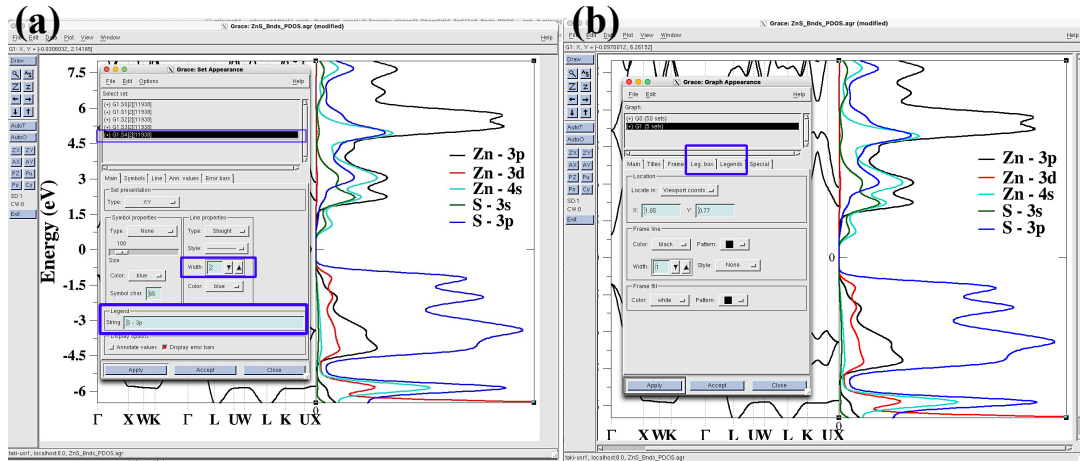


Figure S11. Editing PDOS curves' appearance and legends. (a) Labeling curves (b)Editing legend box.

Drawing a Reference Line at Energy = 0

As seen in all PDOS and band structure plots, a line is drawn at **Energy = 0**, representing the Fermi level (**E_f**), to make it easier to analyze the region near the Fermi energy.

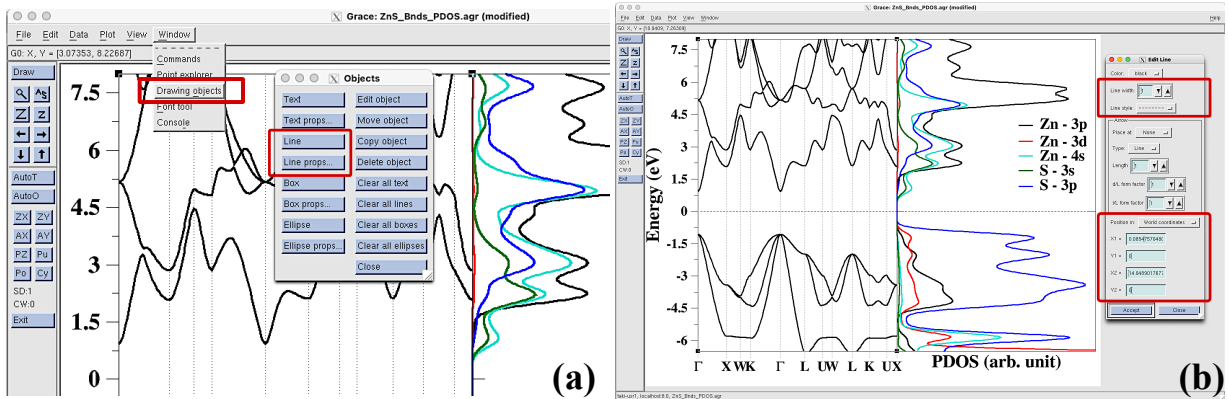


Figure S12. (a) Drawing a reference line at Fermi energy (b) Editing line properties

Steps to Draw the Line (Figure S12):

1. Go to **Window** → **Drawing Objects** → **Line**.
 2. Draw a horizontal line at **Energy = 0**.
 3. Click on the line to open the **Edit Line** box.
 - Adjust the **placement** and **coordinates** to ensure it aligns with **Energy = 0**.
 - Customize the **line style**, **color**, and **size** as needed.
- Click **Apply** to finalize the line placement.

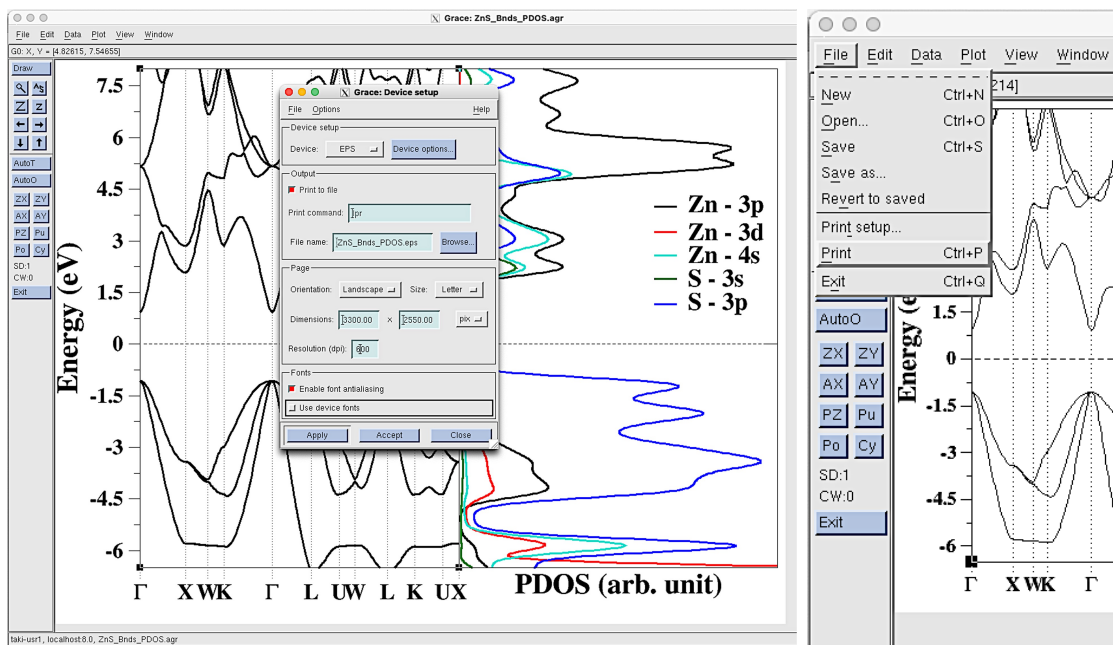


Figure S13. Saving the plot as a high-quality image

S.4.4. Saving the Plot as a High-Quality Image (Figure S13)

After completing the plot and saving the main file in “.agr” format, follow these steps to export the image in high quality:

1. **Set Up Printing:** Go to **File** → **Print Setup** to configure the output settings.
2. **Save as EPS Format:**
 - Save the file in **EPS (Encapsulated PostScript)** format.

- EPS files can be easily converted to **PDF** format, ensuring high resolution suitable for publications or presentations.

3. **Export the Plot:** Go to **File → Print**.

S5. Input File Set for PDOS and Band Analysis per Material System

This section presents the input files and their contents for the 7 material systems analyzed in this study. A sample input file set for Si is included to inspire readers to access the complete dataset in the linked open-access digital repositories Zenodo and GitHub(<https://github.com/bennettlabs-UMBC/Electronic-Band-Structures>) and reproduce the calculations.

S5.1. scf input file for Si:

```
&CONTROL
  calculation = 'scf',
  pseudo_dir = './'
 outdir = './temp',
  prefix = 'Si',
  etot_conv_thr = 1.D-7,
  forc_conv_thr = 2.D-6,
  nstep = 100,
/
&SYSTEM
  ibrav = 2,
  celldm(1) = 10.27974,
  nat = 2,
  ntyp = 1,
  nbnd = 30,
  ecutwfc = 40,
  ecutrho = 320,
  occupations = 'smearing',
  smearing = 'gaussian',
  degauss = 0.005,
  input_dft = 'wc',
/
&ELECTRONS
  electron_maxstep = 150,
  diagonalization = 'david',
  conv_thr = 1.0d-7,
  mixing_beta = 0.2,
/
&IONS
/
&CELL
  press = 0.0,
/
ATOMIC_SPECIES
Si 28.0855 si_pbe_v1.uspp.F.UPF

ATOMIC_POSITIONS {crystal}
Si      0.000    0.000    0.000
Si      0.250    0.250    0.250

K_POINTS {automatic}
10 10 10 0 0 0
```

S5.2. nscf input file for Si:

```
&CONTROL
  calculation = 'nscf',
  pseudo_dir = './',
 outdir = './temp',
  prefix = 'Si',
etot_conv_thr=1.D-7,
forc_conv_thr=2.D-6,
nstep=100,
/
&SYSTEM
  ibrav = 2,
  celldm(1) = 10.27974,
  nat = 2,
  ntyp = 1,
  nbnd = 100,
  ecutwfc = 40,
  ecutrho = 320,
  occupations = 'smearing',
  smearing = 'gaussian',
  degauss = 0.005,
  input_dft='wc',
/
&ELECTRONS
  electron_maxstep = 150,
  diagonalization = 'david',
  conv_thr = 1.0d-7,
  mixing_beta = 0.2,
/
&IONS
/
&CELL
  press = 0.0,
/
ATOMIC_SPECIES
Si 28.0855 si_pbe_v1.uspp.F.UPF

ATOMIC_POSITIONS {crystal}
Si      0.000    0.000    0.000
Si      0.250    0.250    0.250

K_POINTS {automatic}
10 10 10 0 0 0
```

S5.3. bands input file for Si:

```
&CONTROL
  calculation = 'bands',
  pseudo_dir = './',
 outdir = './temp',
  prefix = 'Si',
etot_conv_thr=1.D-7,
forc_conv_thr=2.D-6,
nstep=100,
/
&SYSTEM
  ibrav = 2,
  celldm(1) = 10.27974,
  nat = 2,
```

```

ntyp = 1,
nbnd = 45,
ecutwfc = 40,
ecutrho = 320,
occupations = 'smearing',
smearing = 'gaussian',
degauss = 0.005,
input_dft='wc',
/
&ELECTRONS
  electron_maxstep = 150,
  diagonalization = 'david',
  conv_thr = 1.0d-7,
  mixing_beta = 0.2,
/
&IONS
/
&CELL
  press = 0.0,
/
ATOMIC_SPECIES
Si 28.0855 si_pbe_v1.uspp.F.UPF

ATOMIC_POSITIONS {crystal}
Si      0.000   0.000   0.000
Si      0.250   0.250   0.250

K_POINTS crystal_b
12
  0.0000  0.0000  0.0000  30 !  $\Gamma$  to X
  0.5000  0.0000  0.5000  40 ! X to W
  0.5000  0.2500  0.7500  20 ! W to K
  0.3750  0.3750  0.7500  40 ! K to  $\Gamma$ 
  0.0000  0.0000  0.0000  40 !  $\Gamma$  to L
  0.5000  0.5000  0.5000  30 ! L to U
  0.6250  0.2500  0.6250  20 ! U to W
  0.5000  0.2500  0.7500  20 ! W to L
  0.5000  0.5000  0.5000  30 ! L to K
  0.3750  0.3750  0.7500  20 ! K to U
  0.6250  0.2500  0.6250  30 ! U to X
  0.5000  0.0000  0.5000  30 ! X to  $\Gamma$ 

```

S5.4. dos input file for Si:

```

&dos
prefix='Si'
outdir='./temp/'
Emin = -20.00,
Emax = 20.00,
DeltaE = 0.015,
fildos = 'dos.dat'
/

```

S5.5. PDOS input file for Si:

```
&projwfc
 outdir='./temp/'
prefix='Si'
DeltaE=0.015,
/
```

S4.6. bands input file for Si:

```
&bands
  prefix = 'Si'
  filband = 'bands.dat'
  outdir = './temp',
/
```

S5.6. bands input file for Si:

```
&bands
  prefix = 'Si'
  filband = 'bands.dat'
  outdir = './temp',
/
```

S5.7. plotband input file for Si:

```
bands.dat
-20.00 20.00
bands.xmgr
bands.ps
6.3300
1.00, 6.3300
```

S6. System and Hardware Requirements for DFT Calculations

S6.1. Operating System

- a) **Linux-based HPC clusters:** QE is designed for Linux environments. Ubuntu, CentOS, and Fedora are examples of open-source Linux distributions.
- b) **Windows:** For Windows users, options like Windows Subsystem for Linux (WSL), a feature of the Windows system, or virtual machines, a digitized version of a computer system, allow running Linux and subsequently QE on Windows

- c) **macOS:** QE runs on macOS but may need manual setup with OpenMPI (a tool for running programs across multiple processors for faster computing) and FFTW (a library for handling complex math in scientific calculations).

S6.2. The Computational Power

The computational cost depends on the system and calculation features like symmetry, k-points, surface or bulk calculation, magnetism, and XC functional choice.

System size and structural complexity:

- a) **1–20 atoms** including simple unit cells (Si 2 atoms, diamond 8 atoms), small molecules, high-symmetry bulk structures can run on a standard laptop or desktop (8–16 GB RAM).
- b) **20–100 atoms** including bulk materials with lower symmetry, small supercells, minimal defects. These systems require an advanced system (16–64 GB RAM, 8+ cores).
- c) **100–300 atoms** including surfaces, supercells, defect studies, moderate vacuum demand multi-core systems (64–128 GB RAM, 16+ cores).
- d) **Large systems (> 300 atoms)** including large-scale supercells, amorphous crystal structures, more complicated XC functionals-based calculations need High Performance Computing (HPC) cluster with 128+ GB RAM, 100s–1000s of cores.

S6.3. Computation Settings

- a) **Plane-Wave Cutoff (ecutwfc, ecutrho)** Higher values improve accuracy but increase memory and CPU usage.
- b) Typical ranges: 30–40 Ry (simple materials), 50–80 Ry (oxides, metals), 100+ Ry (hard pseudopotentials).
- c) **K-Point Grid (K_POINTS)** More k-points = Higher accuracy but longer runtime. A $6 \times 6 \times 6$ grid takes $\sim 4 \times$ longer than a $2 \times 2 \times 2$ grid. Bulk systems need fewer k-points than surfaces/slabs.
- d) **Parallelization (npool, ntasks-per-node)** MPI and OpenMP reduce runtime, but scaling depends on the calculation type. SCF and VC-Relax run much faster with more cores, while NSCF and PDOS have limited improvement.

S6.4. DFT Calculation Run Time

Tracking SCF, VC-Relax, NSCF, Bands, and PDOS is fundamental for computational cost analysis. SCF and VC-Relax are the most demanding due to their iterative convergence requirements, while NSCF, Bands, and PDOS depend on k-points and parallelization efficiency. Table S3 provides

- a) **SCF Calculations:**
Small system (few atoms): ~10–30 seconds
Medium system (tens of atoms): ~5–20 minutes
Large system (100+ atoms): Hours to days
- b) **VC-Relax (Geometry Optimization):**
ZnO Relaxation: ~647s (2 nodes, 36 cores)
- c) PbTiO₃ Relaxation: ~19 minutes (2 nodes, 36 cores)
If not parallelized, could take 5–10× longer.

- d) **NSCF / Bands / PDOS:** Faster than SCF but depends on k-point density.
 PbTiO_3 Bands took ~43 minutes, SCF ~17 minutes.
- e) **PDOS** can be as expensive as NSCF, depending on orbital projections.

Table S3. Overview of Computational Performance and Resource Usage

Si-8 Atoms	Nodes	Cores	CPU Time	Run Time	RAM usage per core	SCF Steps
vc-relax	2	36	332.30s	5m36.28s	652.01MB	34
scf	1	48	3.62s	4.41s	232.47 MB	6
nscf	1	48	21.58s	22.76s	501.08 MB	-
bands	1	48	37.80s	41.36s	206.69 MB	-
pdos	1	48	3.18s	4.53s	-	-
GaAs-2 Atoms	Nodes	Cores	CPU Time (s)	Run Time	RAM usage per core	SCF Steps
vc-relax	2	36	33.10s	29.28s	480.93 MB	10
scf	2	36	71.30s	75.73s	708.42 MB	9
nscf	2	36	57.04s	59.59s	482.10 MB	-
bands	2	36	94.83s	99.14s	482.10 MB	-
pdos	2	36	4.16s	5.61s	-	-
ZnS-2 Atoms	Nodes	Cores	CPU Time	Run Time	RAM usage per core	SCF Steps
vc-relax	2	36	21.10s	20.0s	448.33 MB	13
scf	1	48	21.97s	24.21s	433.29 MB	9
nscf	1	48	14.99s	20.21s	333.37 MB	-
bands	1	48	42.70s	46.16s	333.37 MB	-
pdos	1	48	4.24s	5.83s	-	-
ZnO-4 Atoms	Nodes	Cores	CPU Time	Run Time	RAM usage per core	SCF Steps
vc-relax	2	36	10m44.14s	11m40.32s	440.19 MB	23
scf	2	36	14.80s	16.67 s	305.27 MB	10
nscf	2	36	14.99s	20.21s	202.60 MB	-
bands	2	36	13.29s	14.65s	202.60 MB	-
pdos	2	36	2.25s	2.96s	-	-

PbTiO₃- 5 Atoms	Nodes	Cores	CPU Time	Run Time	RAM usage per core	SCF Steps
vc-relax	2	36	17m43.38s	19m5.80s	612.40 MB	22
scf	1	48	1m7.65s	1m14.18s	1014.54 MB	10
nscf	1	48	54.73s	59.26s	769.36 MB	-
bands	1	48	13.29s	14.65s	769.36 MB	-
pdos	1	48	2m39.16s	2m45.38s	-	-
PbO- 4 Atoms	Nodes	Cores	CPU Time	Run Time	RAM usage per core	SCF Steps
vc-relax	2	36	41m27.38s	2h51m	552.12 MB	11
scf	2	36	1m32.47s	4m24.00s	543.55 MB	10
nscf	2	36	49.85s	2m1.23s	330.97 MB	-
bands	2	36	1m40.66s	4m25.32s	330.97 MB	-
pdos	2	36	6.39s	13.31s	-	-
CaCO₃- 20 Atoms	Nodes	Cores	CPU Time	Run Time	RAM usage per core	SCF Steps
vc-relax	1	48	42m9.19s	43m30.97s	4.74GB	22
scf	1	48	1m3.31s	1m7.35s	1022.73 MB	11
nscf	1	48	43.32s	47.25s	645.04 MB	-
bands	1	48	3m52.65s	4m10.19s	645.04 MB	-
pdos	1	48	8.71s	20.65s	-	-

S7. References

1. Flowers, P.; Theopold, K.; Langley, R. *Chemistry 2e*, 2e ed.; Open textbook library; OpenStax: Houston, Texas, 2019.
2. Atkins, P. W.; Jones, L.; Laverman, L. E. *Chemical Principles: The Quest for Insight*, 6. ed., [international ed.]; Freeman: New York, NY, 2013.
3. Atkins, P. W.; De Paula, J. *Physical Chemistry*, 9th ed.; W.H. Freeman: New York, 2010.
4. Miessler, G. L.; Fischer, P. J.; Tarr, D. A. *Inorganic Chemistry*, Fifth edition.; Pearson: Boston, 2014.
5. Vincent, A. *Molecular Symmetry and Group Theory: A Programmed Introduction to Chemical Applications*, 2nd ed.; J. Wiley & sons: Chichester, 2001.
6. Woodward, P. M.; Karen, P.; Evans, J. S. O.; Vogt, T. *Solid State Materials Chemistry*, 1st ed.; Cambridge University Press, 2021. DOI: 10.1017/9781139025348.
7. Hoffmann, R. *Solids and Surfaces: A Chemist's View of Bonding in Extended Structures*, Print on demand der Ausg. 1988.; Wiley-VCH: New York, NY, 2002.
8. Hoffmann, R. A Chemical and Theoretical Approach to Bonding at Surfaces. *J. Phys.: Condens. Matter* **1993**, 5 (33A), A1–A16. DOI: 10.1088/0953-8984/5/33A/001.

9. Hoffmann, R. How Chemistry and Physics Meet in the Solid State. *Angew. Chem. Int. Ed. Engl.* **1987**, 26 (9), 846–878. DOI: 10.1002/anie.198708461.
10. Mattsson, A. E.; Schultz, P. A.; Desjarlais, M. P.; Mattsson, T. R.; Leung, K. Designing Meaningful Density Functional Theory Calculations in Materials Science—a Primer. *Modelling Simul. Mater. Sci. Eng.* **2004**, 13 (1), R1–R31. DOI: 10.1088/0965-0393/13/1/R01.
11. Payne, M. C.; Teter, M. P.; Allan, D. C.; Arias, T. A.; Joannopoulos, J. D. Iterative Minimization Techniques for *Ab Initio* Total-Energy Calculations: Molecular Dynamics and Conjugate Gradients. *Rev. Mod. Phys.* **1992**, 64 (4), 1045–1097. DOI: 10.1103/RevModPhys.64.1045.
12. Sholl, D. S.; Steckel, J. A. *Density Functional Theory: A Practical Introduction*; Wiley: Hoboken, N.J, 2009.
13. Kittel, C.; Kittel, U. C. *Introduction to Solid State Physics*; Wiley, 1976.
14. Martin, R. M. *Electronic Structure: Basic Theory and Practical Methods*, 1st ed.; Cambridge University Press, 2004. DOI: 10.1017/CBO9780511805769.
15. Gražulis, S.; Chateigner, D.; Downs, R. T.; Yokochi, A. F. T.; Quirós, M.; Lutterotti, L.; Manakova, E.; Butkus, J.; Moeck, P.; Le Bail, A. Crystallography Open Database – an Open-Access Collection of Crystal Structures. *J Appl Crystallogr* **2009**, 42 (4), 726–729. DOI: 10.1107/S0021889809016690.
16. Gražulis, S.; Daškevič, A.; Merkys, A.; Chateigner, D.; Lutterotti, L.; Quirós, M.; Serebryanaya, N. R.; Moeck, P.; Downs, R. T.; Le Bail, A. Crystallography Open Database (COD): An Open-Access Collection of Crystal Structures and Platform for World-Wide Collaboration. *Nucleic Acids Res.* **2012**, 40 (D1), D420–D427. DOI: 10.1093/nar/gkr900.
17. Jain, A.; Ong, S. P.; Hautier, G.; Chen, W.; Richards, W. D.; Dacek, S.; Cholia, S.; Gunter, D.; Skinner, D.; Ceder, G.; Persson, K. A. Commentary: The Materials Project: A Materials Genome Approach to Accelerating Materials Innovation. *APL Materials* **2013**, 1 (1), 011002. DOI: 10.1063/1.4812323.
18. k, J. Computer Programs for Drawing Crystal Shapes and Atomic Structures. *Rocks & Minerals* **2018**, 93 (1), 60–64. DOI: 10.1080/00357529.2018.1383832.
19. Momma, K.; Izumi, F. VESTA 3 for Three-Dimensional Visualization of Crystal, Volumetric and Morphology Data. *J Appl Crystallogr* **2011**, 44 (6), 1272–1276. DOI: 10.1107/S0021889811038970.
20. Kokalj, A. XCrySDen—a New Program for Displaying Crystalline Structures and Electron Densities. *Journal of Molecular Graphics and Modelling* **1999**, 17 (3–4), 176–179. DOI: 10.1016/S1093-3263(99)00028-5.
21. Palmer, D. C. Visualization and Analysis of Crystal Structures Using CrystalMaker Software. *Zeitschrift für Kristallographie – Cryst. Mater.* **2015**, 230 (9–10), 559–572. DOI: 10.1515/zkri-2015-1869.
22. Setyawan, W.; Curtarolo, S. High-Throughput Electronic Band Structure Calculations: Challenges and Tools. *Computational materials science* **2010**, 49 (2), 299–312.
23. Hinuma, Y.; Pizzi, G.; Kumagai, Y.; Oba, F.; Tanaka, I. Band Structure Diagram Paths Based on Crystallography. *Computational Materials Science* **2017**, 128, 140–184. DOI: 10.1016/j.commatsci.2016.10.015.
24. Janert, P. K. *Gnuplot in Action: Understanding Data with Graphs*; Simon and Schuster, 2016.
25. Racine, J. Gnuplot 4.0: A Portable Interactive Plotting Utility. *J of Applied Econometrics* **2006**, 21 (1), 133–141. DOI: 10.1002/jae.885.
26. Moore, W. J.; Pauling, L. The Crystal Structures of the Tetragonal Monoxides of Lead, Tin, Palladium, and Platinum. *J. Am. Chem. Soc.* **1941**, 63 (5), 1392–1394. DOI: 10.1021/ja01850a074.
27. Geldasa, F. T.; Kebede, M. A.; Shura, M. W.; Hone, F. G. Density Functional Theory Study of Different Metal Dopants Influence on the Structural and Electronic Properties of a Tetragonal α -PbO. *AIP Advances* **2022**, 12 (11), 115302. DOI: 10.1063/5.0121828.
28. Payne, D. J.; Egddell, R. G.; Law, D. S. L.; Glans, P.-A.; Learmonth, T.; Smith, K. E.; Guo, J.; Walsh, A.; Watson, G. W. Experimental and Theoretical Study of the Electronic Structures of α -PbO and β -PbO₂. *J. Mater. Chem.* **2007**, 17 (3), 267–277. DOI: 10.1039/B612323F.

29. Payne, D. J.; Egdell, R. G.; Walsh, A.; Watson, G. W.; Guo, J.; Glans, P.-A.; Learmonth, T.; Smith, K. E. Electronic Origins of Structural Distortions in Post-Transition Metal Oxides: Experimental and Theoretical Evidence for a Revision of the Lone Pair Model. *Phys. Rev. Lett.* **2006**, *96* (15), 157403. DOI: 10.1103/PhysRevLett.96.157403.
30. Cohen, R. E. Origin of Ferroelectricity in Perovskite Oxides. *Nature* **1992**, *358* (6382), 136–138. DOI: 10.1038/358136a0.
31. Bennett, J. W.; Garrity, K. F.; Rabe, K. M.; Vanderbilt, D. Hexagonal ABC Semiconductors as Ferroelectrics. *Phys. Rev. Lett.* **2012**, *109* (16), 167602. DOI: 10.1103/PhysRevLett.109.167602.
32. Khan, A. C.; Cook, A. S.; Leginze, J. A.; Bennett, J. W. Developing New Antiferroelectric and Ferroelectric Oxides and Chalcogenides within the A_2BX_3 Family. *Journal of Materials Research* **2022**, *37* (1), 346–359. DOI: 10.1557/s43578-021-00410-3.
33. Bhatti, H. S.; Hussain, S. T.; Khan, F. A.; Hussain, S. Synthesis and Induced Multiferroicity of Perovskite $PbTiO_3$; a Review. *Applied Surface Science* **2016**, *367*, 291–306. DOI: 10.1016/j.apsusc.2016.01.164.
34. Chchiyai, Z.; El Bachraoui, F.; Tamraoui, Y.; Mehdi Haily, E.; Bih, L.; Lahmar, A.; El Marssi, M.; Alami, J.; Manoun, B. Effect of Cobalt Doping on the Crystal Structure, Magnetic, Dielectric, Electrical and Optical Properties of $PbTi_{1-x}Co_xO_{3-\delta}$ Perovskite Materials. *Journal of Alloys and Compounds* **2022**, *927*, 166979. DOI: 10.1016/j.jallcom.2022.166979.
35. Arras, R.; Gostreau, J.; Zhao, H. J.; Paillard, C.; Yang, Y.; Bellaiche, L. Rashba-like Spin-Orbit and Strain Effects in Tetragonal $PbTiO_3$. *Phys. Rev. B* **2019**, *100* (17), 174415. DOI: 10.1103/PhysRevB.100.174415.
36. Heimann, J. E.; Tucker, J. D.; Huff, L. S.; Kim, Y. R.; Ali, J.; Stroot, M. K.; Welch, X. J.; White, H. E.; Wilson, M. L.; Wood, C. E.; Gates, G. A.; Rosenzweig, Z.; Bennett, J. W. Density Functional Theory (DFT) as a Nondestructive Probe in the Field of Art Conservation: Small-Molecule Adsorption on Aragonite Surfaces. *ACS Appl. Mater. Interfaces* **2022**, *14* (11), 13858–13871. DOI: 10.1021/acsami.1c23695.
37. Medeiros, S. K.; Albuquerque, E. L.; Maia, F. F.; Caetano, E. W. S.; Freire, V. N. Structural, Electronic, and Optical Properties of $CaCO_3$ Aragonite. *Chemical Physics Letters* **2006**, *430* (4–6), 293–296. DOI: 10.1016/j.cplett.2006.08.133.
38. De Villiers, J. P. Crystal Structures of Aragonite, Strontianite, and Witherite. *American Mineralogist: Journal of Earth and Planetary Materials* **1971**, *56* (5–6), 758–767.
39. Dickens, B.; Bowen, J. S. Refinement of the Crystal Structure of the Aragonite Phase of $CaCO_3$. *J. RES. NATL. BUR. STAN. SECT. A* **1971**, *75A* (1), 27. DOI: 10.6028/jres.075A.004.